STRUCTURAL EFFECTS THROUGH NUCLEAR CHARGE RADIUS IN MASS ASYMMETRIC COLLISIONS*

Sangeeta

School of Physics and Materials Science, Thapar University, Patiala-147004, India

Varinderjit Kaur

Department of Physics, Mata Gujri College, Fatehgarh Sahib-140406, India

(Received December 14, 2016)

The structural effects through nuclear charge radius on the multifragmentation and nuclear stopping have been studied for mass symmetric and asymmetric collisions using Isospin-dependent Quantum Molecular Dynamics (IQMD) model. Our analysis shows that the role of increase in radius is more pronounced in mass symmetric collisions compared to asymmetric collisions. Moreover, we explicitly studied the influence of radius on the contribution of projectile and target nuclei in the nuclear stopping.

DOI:10.5506/APhysPolB.48.623

1. Introduction

In heavy-ion collisions (HICs), the multifragmentation and nuclear stopping essentially depend on incident energy (E), collision geometry (b), mass of the colliding nuclei ($A_{\rm P}, A_{\rm T}$) and mass asymmetry $\eta = |A_{\rm T} - A_{\rm P}/A_{\rm T} + A_{\rm P}|$ [1]. Here, $A_{\rm T}$ and $A_{\rm P}$ are mass numbers of target and projectile nuclei respectively. Apparently, $\eta = 0.0$ corresponds to completely symmetric collisions and the distribution of fragments is spherical, whereas asymmetric collisions having non-zero η lead to non-spherical distribution at central collision geometry. The reaction dynamics and the by-products are entirely different for reactions with different values of η [2]. The nuclear charge radii is the another entrance channel parameter which is essential to initialize the nuclear matter in HICs and it affects the reaction dynamics very drastically [3, 4].

* Presented at the Zakopane Conference on Nuclear Physics "Extremes of the Nuclear Landscape", Zakopane, Poland, August 28–September 4, 2016.

Although the dynamics of symmetrically heavy nuclei is prominently studied with different parameterizations of nuclear charge radii, unfortunately, no attention is being paid to study the structural effects via nuclear charge radii in the dynamics of mass asymmetric collisions. We want to study the comparable role of different nuclear charge radii parameterizations on the fragmentation and nuclear stopping in mass symmetric and asymmetric collisions. The global parameter of nuclear stopping *i.e.* anisotropy ratio, is defined as: $\langle R\rangle = (2/\pi)([\sum_i^{A_{\rm tot}} |p_\perp(i)|]/[\sum_i^{A_{\rm tot}} |p_\parallel(i)|])$. The transverse and longitudinal momentum of the $i^{\rm th}$ particle are $p_\perp(i) = \sqrt{p_x^2(i)+p_y^2(i)}$ and $p_\parallel(i) = p_z(i)$ respectively. $A_{\rm tot} = A_{\rm P} + A_{\rm T}$ is the total mass of the nuclear system.

Out of numerous parameterizations of nuclear charge radii, we chose four parameterizations in such a way that the calculated radius of nuclei follows the pattern: $R_{\rm LDM}$ [5] $< R_{\rm NGO}$ [6] $< R_{\rm PP}$ [7] $< R_{\rm RR}$ [8], and the study of structural effects via increase in nuclear radius can be kept in a systematic way. The detailed description of these parameterizations are in Refs. [3–9]. The present calculations have been preformed within the framework of Isospin-dependent Quantum Molecular Dynamics (IQMD) model [10].

2. Results and discussion

The simulations have been carried out over the entire collision geometry for the reactions of $^{50}_{20}$Ca+$^{50}_{20}$Ca ($\eta = 0.0$) and $^{14}_{7}$N+$^{86}_{36}$Kr ($\eta = 0.7$) ($A_{\rm tot} =$ 100 units) using IQMD model [10] at incident energy of 100 MeV/nucleon. Figure 1 displays the multiplicity of free nucleons (FNs, $A = 1$) (left panels) and light-mass fragments (LMFs, $2 \le A \le 4$) (right panels) as a function of nuclear stopping for mass symmetric (upper panels) and asymmetric (lower panels) collisions at six collision geometries described by various symbols and for four different nuclear charge radii parameterizations described by various lines. One can observe that the multiplicity and the nuclear stopping decreases with the increase in scaled impact parameter *i.e.* $\hat{b} = b/b_{\rm max}$, where $b_{\rm max} = (R_{\rm P} + R_{\rm T})$ fm ($R_{\rm P}$ and $R_{\rm T}$ are radii of target and projectile nuclei respectively). The correlation curve of multifragmentation and nuclear stopping reveals that the higher is the nuclear stopping, the higher will be the fragmentation and, therefore, the curve increases monotonically with decrease in $\hat{b}$ for all radii parameterizations. For mass symmetric collisions, if we initialize the nucleus with relatively larger radii (*i.e.* $R_{\rm LDM}$ to other three parameterizations), the multiplicity of fragments increases and the nuclear stopping decreases [4]. This is because with the increase in radius, $p_\perp(i)$ and $p_\parallel(i)$ increase and, moreover, the increment in longitudinal momentum is higher than the transverse momentum. This observation also holds true for mass asymmetric collisions.

The ratio of change in multiplicity of fragments as well as the nuclear stopping to the change in nuclear radii of the colliding nuclei (switching from $R_{\rm LDM}$ to $R_{\rm RR}$) is greater for mass symmetric collisions compared to mass asymmetric collisions, while the total mass number is the same in both types of collisions. This is because of involvement of smaller projectile nucleus in mass asymmetric collisions.

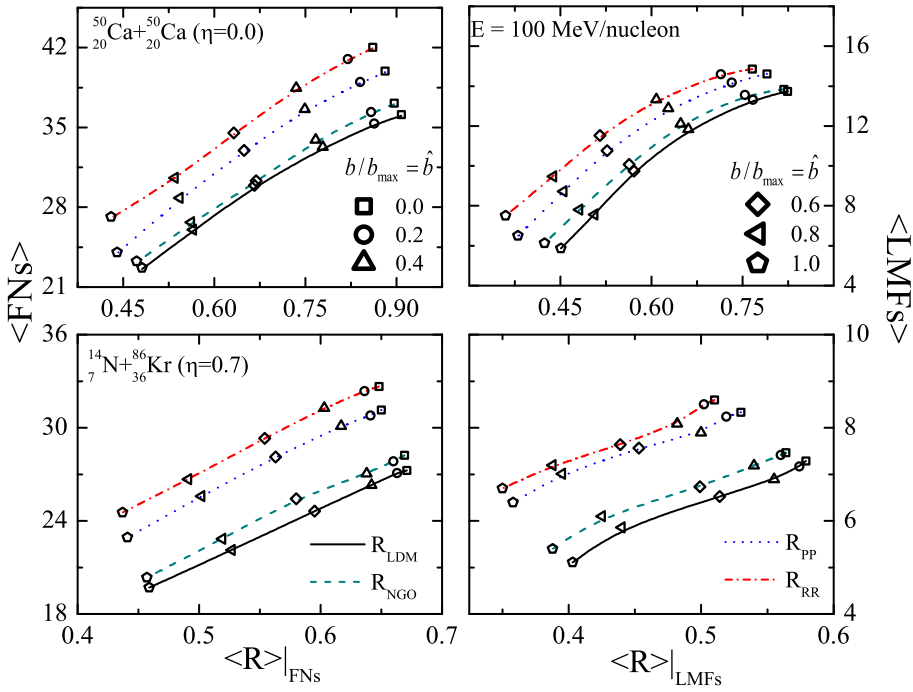

Fig. 1. Multiplicity of FNs (left panels) and LMFs (right panels) as a function of nuclear stopping for mass symmetric (upper panels) and asymmetric (lower panels) nuclear reactions with $A_{\rm tot} = 100$ units at $E = 100$ MeV/nucleon.

The percentage increment in nuclear radius from $R_{\rm LDM}$ to $R_{\rm RR}$ is 28.5% for $^{14}_{7}$N and 10% for $^{86}_{36}$Kr nucleus. It shows that the effect of radius on smaller projectile and heavier target will be different. Therefore, as a next step, we display in Fig. 2 the structural effects on nuclear stopping due to projectile (left panel) and target (right panel) nucleus explicitly for mass asymmetric collisions of $^{14}_{7}$N+$^{86}_{36}$Kr. The figure reveals that the contribution of projectile nucleus ($^{14}_{7}$N) is more compared to target nucleus ($^{86}_{36}$Kr) in nuclear stopping. Furthermore, we observe that the structural effects via nuclear charge radius are more pronounced in nuclear stopping due to relatively smaller nucleus compared to larger nucleus. This is because, in mass asymmetric collisions,

most of the nuclear matter of heavier target nucleus do not participate in the collision process. At $\hat{b} = 0.0$, the projectile nucleus completely emerges into target nucleus and at $\hat{b} = 1.0$, the projectile and target barely touch each other. So, there is no role of radius on nuclear stopping due to projectile nuclei at these collision geometry.

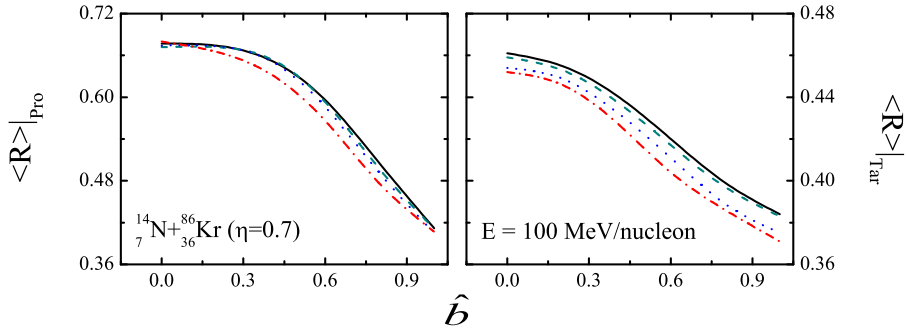

Fig. 2. Collision geometry dependence of nuclear stopping due to projectile (left panel) and target (right panel) nuclei for the reaction of $^{14}_{7}$N+$^{86}_{36}$Kr ($\eta = 0.7$) at $E = 100$ MeV/nucleon. Lines have the same meaning as in Fig. 1.

3. Summary

In summary, we observe that the influence of nuclear charge radii parameterizations on the correlation between multifragmentation and nuclear stopping is more pronounced in mass symmetric collisions compared to asymmetric collisions. Moreover, the structural effects via nuclear charge radii parameterizations are more prominent for nuclear stopping due to smaller projectile nucleus compared to heavier target nucleus.

The financial support from the Department of Science and Technology (DST), Government of India in terms of INSPIRE-fellowship (grant No. DST/INSPIRE/03/2014/000234) and Young Scientist Award under the SERC Fast Track Scheme, wide letter No. SR/FTP/PS-020/2012 is gratefully acknowledged. We are also thankful to Prof. Rajeev K. Puri for giving access to his various computer programs for the current work.

REFERENCES

[1] J. Singh, R.K. Puri, *J. Phys. G: Nucl. Part. Phys.* **27**, 2091 (2001).

[2] V. Kaur, S. Kumar, *J. Phys. G: Nucl. Part. Phys.* **39**, 085114 (2012); *Phys. Rev. C* **81**, 064610 (2010).

[3] S. Gautam, *Phys. Rev. C* **88**, 057603 (2013).

[4] Sangeeta, A. Jain, S. Kumar, *Nucl. Phys. A* **927**, 220 (2014); Sangeeta, *Acta Phys. Pol. B* **47**, 991 (2016).

[5] A. Bohr, B. Mottelson, *Nuclear Structure, Volume I*, W.A. Benjamin Inc., New York, Amsterdam 1969, p. 268.

[6] H. Ngô, Ch. Ngô, *Nucl. Phys. A* **348**, 140 (1980).

[7] B. Nerlo-Pomorska, K. Pomorski, *Z. Phys. A* **348**, 169 (1994).

[8] G. Royer, R. Rousseau, *Eur. Phys. J. A* **42**, 541 (2009).

[9] I. Dutt, R.K. Puri, *Phys. Rev. C* **81**, 064609 (2010).

[10] C. Hartnack *et al.*, *Eur. Phys. J. A* **1**, 151 (1998); C. Hartnack *et al.*, *Phys. Rep.* **510**, 119 (2012).